文章编号: 1001－2060(2008)04－0413－04

二氧化碳气体辐射特性宽带 k 分布模型

尹雪梅, 刘林华, 李炳熙
(哈尔滨工业大学 能源科学与工程学院, 黑龙江 哈尔滨 150001)

摘　要: 建立了一种新的宽带 k 分布模型, 从高温气体数据库 HITEMP 得到二氧化碳气体光谱辐射特性参数, 用关联式拟合了其主要谱带的吸收系数。用该模型计算了二氧化碳的辐射热流, 与逐线计算、统计窄带模型、窄带 k 分布模型和全光谱 k 分布模型作了比较, 结果表明: 对等温气体, 提出的宽带 k 分布模型和逐线计算结果吻合很好, 比全光谱 k 分布模型更准确。如果积分格式选取合适, 宽带 k 分布模型比统计窄带模型精度高, 和窄带 k 分布模型的精度相当。对灰壁面平板间的非等温气体, 宽带 k 分布模型和逐线计算结果相比误差在 10% 左右, 大大提高了气体辐射特性的计算精度和计算速度。

关　键　词: 二氧化碳; 宽带 k 分布模型; 辐射热流
中图分类号: TK124　　文献标识码: A

引　言

二氧化碳是燃料燃烧的主要产物之一, 其辐射计算在工程应用中具有重要意义。为了准确计算辐射必须考虑二氧化碳的非灰辐射特性。气体分子在一定数目的振动－旋转谱带间吸收和发射辐射, 每个谱带又包含成千上万的谱线, 这些光谱线导致在整个光谱上吸收系数剧烈变化。逐线计算(LBL)是最准确的[1], 但需要分子气体每条谱线的详细光谱特性参数, 包括谱线位置、谱线强度、谱线半宽和谱线跃迁能级能量等。以 HITEMP(2000)数据库为例[2], CO_2 有 1 032 269 条谱线。由于其计算量巨大, 一般只将逐线计算结果作为检验其它模型的准确度和有效性的基准解。在工程应用中, 综合考虑精度和计算速度, 常对二氧化碳的 6 个振动－旋转谱带分别进行计算, 得到宽谱带模型。传统宽谱带模型(EWB)是将小波数间隔内的平均吸收系数重新排列后得到的近似关系式[3], 误差很大, 且因其用谱带总吸收率表示辐射特性, 和路径长度有关, 只能用射线踪迹法求解辐射传递方程, 适用于黑体壁面内非散射介质。

气体辐射特性计算只占整个辐射计算的小部分, 应尽可能地提高其计算速度及扩大与辐射传递方程求解方法的兼容性。k 分布模型用吸收系数表示辐射特性, 能用任意辐射传递方程求解方法求解, 所以近些年许多学者在这方面作了研究。窄带 k 分布模型对非等温介质需要计算不同温度下的吸收系数然后重排[4~5], 对计算机容量要求高且计算时间长。Modest 等人提出了全光谱 k 分布模型(FSK)[6~9], 使 k 分布模型能在整个谱带应用, 但由于谱带范围太大, 温度对不同波数区间影响不同, 导致其对非等温介质误差很大。现有的宽谱带 k 分布模型基本都是建立在指数宽谱带模型基础上[10~12], 加上一些假设, 使其精度和适用性受到限制。综合考虑计算精度和计算速度, 建立了一种新的宽带 k 分布模型, 从高温气体的数据库 HITEMP 得到气体光谱特性参数, 能快速准确计算二氧化碳的辐射换热, 且与任意辐射传递方程求解方法相容。

1　宽带 k 分布模型

在小的谱带间隔内普朗克函数基本不变, 则辐射强度和热流只受气体吸收系数影响, 而剧烈变化的吸收系数值在很小波数间隔内多次相同, 每次都得到相同的辐射强度和热流。k 分布思想就是: 将吸收系数排列成平滑单调上升的函数, 对相同的吸收系数就只进行一次强度计算。因其用吸收系数表示辐射特性, 故能与任意辐射传递方程求解方法相容。

考察二氧化碳气体的重要谱带在不同温度下的普朗克函数, 可以看出: 最大普朗克函数 $I_{b\eta\max}$ 和最小普朗克函数 $I_{b\eta\min}$ 差值与谱带中心波数 η_0 的普朗克函数 $I_{b\eta 0}$ 的比值, $\mathrm{diff} = (I_{b\eta\max} - I_{b\eta\min}) \times 100\% / I_{b\eta 0}$, 最大可能达到 220% 以上。由于宽谱带的波数间距较大, 普朗克函数变化较大, 假设普朗克函数不变会导致很大的误差。为了克服上述缺点, 在 k 分

收稿日期: 2007－07－13;　修订日期: 2007－08－31
基金项目: 国家自然科学基金资助项目(50425619, 50636010)
作者简介: 尹雪梅(1979－), 女, 四川资中人, 哈尔滨工业大学博士研究生。

布模型中引入普朗克加权函数$f(T, k)$:

$$f(T, k) = \frac{1}{I_{b\Delta\eta}}\int_{\Delta\eta} I_{b\eta}(T)\,\delta(k-\kappa_\eta)\mathrm{d}\eta \tag{1}$$

式中:$I_{b\Delta\eta}$、$I_{b\eta}$—整个谱带总的黑体强度和光谱黑体强度;κ_η—光谱吸收系数;$\delta(k-\kappa_\eta)$—Dirac-delta 函数。在不考虑散射情况下,光谱辐射传递方程为:

$$\mathrm{d}I_\eta/\mathrm{d}s = \kappa_\eta I_{b\eta} - \kappa_\eta I_\eta \tag{2}$$

其漫射边界条件为:

$$I_\eta = I_{w\eta} = \varepsilon_w I_{bw\eta} + (1-\varepsilon_w)\frac{1}{\pi}\int_{\hat{n}\cdot\hat{s}<0} I_\eta\,|\hat{n}\cdot\hat{s}|\,\mathrm{d}\Omega \tag{3}$$

在式(2)和式(3)的两边乘 $\delta(k-\kappa_\eta)$,然后对整个谱带积分,再除吸收系数 k 的几率分布函数 $f(T, k)$,得:

$$\mathrm{d}I_g/\mathrm{d}s = k(I_{b\Delta\eta} - I_g) \tag{4}$$

$$I_g = I_{wg} = \varepsilon_w I_{bw} + (1-\varepsilon_w)\frac{1}{\pi}\int_{\hat{n}\cdot\hat{s}<0} I_g\,|\hat{n}\cdot\hat{s}|\,\mathrm{d}\Omega \tag{5}$$

上述式中:

$$I_g = \int_{\Delta\eta} I_\eta\,\delta(k-\kappa_\eta)\mathrm{d}\eta/f(T, k) \tag{6}$$

其中累积分布函数 $g(T, k)$定义为:

$$g(T, k) = \int_0^k f(T, k)\mathrm{d}k \tag{7}$$

从而谱带总辐射强度可以表示为:

$$I = \int_{\Delta\eta} I_\eta \mathrm{d}\eta = \int_0^1 I_g \mathrm{d}g \tag{8}$$

2 宽带 k 分布模型的吸收系数

式(8)常用 Gauss 型的积分方法来计算,其中 7 点 Gauss-Lobatto 积分应用最广泛,考虑到波数间隔较大,本文还采用了 12 点 Gauss-Lobatto 积分:

$$I = \sum_{i=1}^{N} w_i I_{g_i} \tag{9}$$

式中:N—积分点数;w_i—求积的权。从高温气体数据库 HITEMP 获取 CO_2 的光谱特性参数,得到其在不同温度下的吸收系数后,在 CO_2 的 6 个重要谱带上应用前面提出的宽带 k 分布模型,最后用 6 次多项式拟合得到了 CO_2 重要谱带 Gauss 积分点对应的吸收系数。多项式函数形式为:

$$k(g_i) = x(a + bT + cT^2 + dT^3 + eT^4 + fT^5 + hT^6) \tag{10}$$

式中:$k(g_i)$—Gauss 积分点对应的吸收系数;T—气体温度;x—CO_2 体积浓度;a、b、c、d、e、f、h—多项式系数。

3 模型检验与分析

为了检验宽带 k 分布模型的有效性,下面计算 N_2—CO_2 混合物的局部辐射热流,并与逐线计算、窄带 k 分布模型和全光谱 k 分布模型进行比较。逐线计算取波数间距为 $\delta\eta = 0.01\ \mathrm{cm}^{-1}$,窄带模型计算取波数间距为 $\Delta\eta = 25\ \mathrm{cm}^{-1}$。全光谱 k 分布模型采用 12 点 Gauss-Lobatto 积分。以逐线计算作为基准,各模型的误差定义为:

$$\mathrm{err} = \int_0^L |q_{\mathrm{model}} - q_{\mathrm{LBL}}|\,\mathrm{d}x \times 100\% / \int_0^L |q_{\mathrm{LBL}}|\,\mathrm{d}x \tag{11}$$

3.1 算例 1

考虑两无限大平板间的一等温 N_2—CO_2 气体层,平板为黑体且温度均为 0 K。气体总压力为 p = 10 kPa,CO_2 分压力为 $p_{CO_2} = 0.1p$,温度 T = 1 500 K,平板间距为 L。沿气体层厚度方向分为 200 个单元,角度分为 20 个单元立体角。图 1 和图 2 分别给出了 L = 0.01 m 和 L = 1 m 时等温 CO_2 总的局部辐射热流。表 1~表 3 给出了 CO_2 各主要谱带的热流计算误差。表 1 和表 2 表明:对等温气体,本文提出的宽带 k 分布模型结果和逐线计算结果吻合很好,各主要谱带的计算误差基本都小于 0.5%,而窄带 k 分布模型的误差在 0.7%左右。从表 3 可以看出 CO_2 总热流的计算误差:统计窄带模型的计算误差基本在 2%左右,窄带 k 分布模型的误差小于 0.5%,7 点和 12 点宽带 k 分布模型的误差分别在 2%和 0.2%左右,而全光谱 k 分布模型的误差高达 8%。综合表中数据和以上分析得出以下结论:宽带 k 分布模型比全光谱 k 分布模型准确,12 点 Gauss-Lobatto 求积结果比 7 点 Gauss-Lobatto 求积结果更准确。12 点 Gauss-Lobatto 求积结果比统计窄带模型精度高,和窄带 k 分布模型的精度相当。

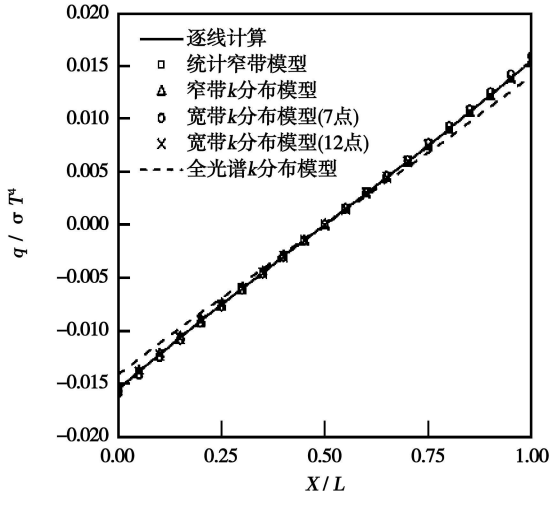

图 1 L = 0.01 m 时等温 CO_2 局部辐射热流

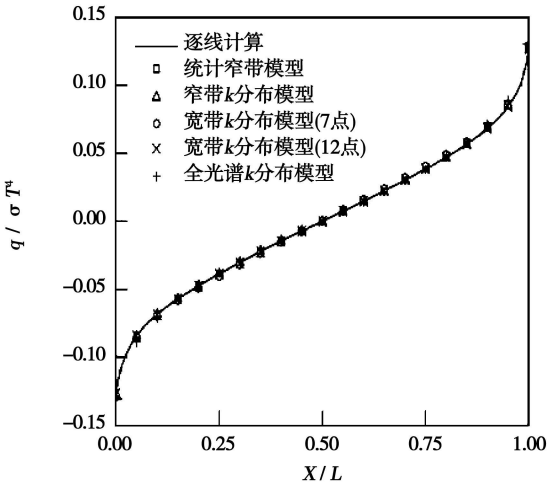

图 2　$L=1$ m 时等温 CO_2 局部辐射热流

表 1　$L=0.01$ m 时等温 CO_2 主要谱带辐射热流的计算误差　(%)

谱带/μm	统计窄带模型	窄带 k 分布模型	宽带 k 分布模型(7 点)	宽带 k 分布模型(12 点)
2.0	0.104 7	0.827 6	0.459 7	0.312 4
2.7	0.195 9	0.803 2	0.423 9	0.173 1
4.3	2.118 7	0.419 4	2.548 5	0.190 4
9.4	0.120 8	0.691 7	0.090 9	0.048 8
10.4	0.146 7	0.870 6	0.141 3	0.108 2
15	1.582 2	0.810 8	4.209 6	0.847 8

表 2　$L=1$ m 时主要谱带辐射热流的计算误差　(%)

谱带/μm	统计窄带模型	窄带 k 分布模型	宽带 k 分布模型(7 点)	宽带 k 分布模型(12 点)
2.0	0.082 4	0.758 6	0.272 2	0.229 6
2.7	2.411 2	0.535 3	0.624 9	0.400 9
4.3	0.326 6	0.872 1	7.355 6	0.164 1
9.4	0.614 3	0.574 4	0.268 4	0.158 8
10.4	0.464 5	0.736 6	0.321 7	0.172 7
15	1.628 8	0.425 1	0.689 1	0.102 0

表 3　等温 CO_2 总热流的计算误差　(%)

	统计窄带模型	窄带 k 分布模型	宽带 k 分布模型(7 点)	宽带 k 分布模型(12 点)	全光谱 k 分布模型
$L=0.01$ m	1.971 3	0.455 7	2.176 6	0.181 4	8.658 3
$L=1$ m	1.553 6	0.117 4	2.589 9	0.264 8	3.166 8

3.2　算例 2

由于"热线"的存在, 关联 k 假设在大的温差情况下会失效。且由于宽带 k 分布波数间距较大, 不同的波数区间温度对吸收系数的影响不同, 关联 k 假设可能会导致很大误差。为了进一步检验前面提出的宽带 k 分布模型, 将其用于灰壁面间非等温 N_2—CO_2 气体层。壁面发射率 $\varepsilon_w=0.8$, 温度为抛物线型, 即:

$$T=4(T_w-T_c)\left(\frac{z}{L}-\frac{1}{2}\right)^2+T_c \qquad (12)$$

平板间距 $L=10$ m, 壁面温度 $T_w=500$ K, 中心温度 $T_c=1\,500$ K, 总压力 $p=101.325$ kPa, 二氧化碳分压为: $p_{CO_2}=0.1p$。沿气体层厚度方向分 200 个单元, 角度分 20 个单元立体角。宽带 k 分布模型采用 12 点 Gauss-Lobatto 积分, 用拟合式得到 $k(g_i)$。全光谱 k 分布模型的参考温度取普朗克平均温度。图 3 给出了 4.3 和 2.7 μm 谱带局部辐射热流的分布。表 4 给出了非等温条件下, 各 k 分布模型的计算误差。除 4.3 μm 谱带误差稍大些达到了 17%外, 在其它谱带上宽带 k 分布模型和逐线计算结果相比误差基本在 10%左右。对于辐射总热流, 窄带 k 分布模型、宽带 k 分布模型和全光谱 k 分布模型的误差分别为: 2.91、12.29 和 30.93。很明显宽带 k 分布模型比全光谱 k 分布模型精度高得多, 同时表 5 所示宽带 k 分布模型计算时间远比窄带 k 分布模型和全光谱 k 分布模型短。

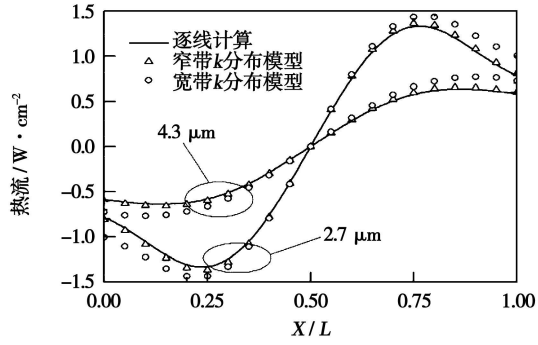

图 3　非等温 CO_2 谱带局部辐射热流

表 4　非等温 CO_2 主要谱带热流的计算误差 (%)

谱带/μm	窄带 k 分布模型	宽带 k 分布模型
2.0	2.86	3.64
2.7	2.79	11.15
4.3	3.14	17.49
9.4	2.59	10.96
10.4	2.33	10.21
15	3.69	13.63

表 5 非等温 CO_2 总热流的计算时间 (s)

逐线计算	窄带 k 分布模型	宽带 k 分布模型	全光谱 k 分布模型
30 192	16 376	26	280

为了提高宽带 k 分布模型的计算精度,可以将谱带适当细分。将对辐射热流起主要作用的 4.3 和 2.7 μm 细分。4.3 μm 分成 1 950~2 100 cm^{-1}、2 100~2 400 cm^{-1}和 2 400~2 450 cm^{-1} 3 个区间,误差可减小到 11.02%, 2.7 μm 分成 3 300~3 470 cm^{-1}、3 470~3 770 cm^{-1}和 3 770~3 800 cm^{-1}3 个区间,误差可减小到 6.99%,总热流的误差可减小到 8.38%。

4 结 论

针对二氧化碳气体建立了一种新的宽带 k 分布模型,从高温气体数据库 HITEMP 得到气体光谱辐射特性参数,得到 CO_2 的 6 个重要谱带不同温度下 Gauss 积分点对应的吸收系数,并用 6 次多项式拟合了谱带的吸收系数。用该模型计算了 N_2-CO_2 气体层的局部辐射热流,与逐线计算、统计窄带模型,窄带 k 分布模型、全光谱 k 分布模型作了比较。结果表明:对等温气体,本文提出的宽带 k 分布模型结果和逐线计算结果吻合很好,比全光谱 k 分布模型更准确。12 点 Gauss-Lobatto 求积结果比 7 点 Gauss-Lobatto 求积结果准确。12 点 Gauss-Lobatto 求积结果比统计窄带模型精度高,和窄带 k 分布模型的精度相当;对灰壁面平板间的非等温气体,宽带 k 分布模型和逐线计算结果相比误差基本在 10%左右,比全光谱 k 分布模型准确,同时计算时间远比窄带 k 分布模型和全光谱 k 分布模型短。将谱带适当细分可以进一步提高计算精度。宽带 k 分布模型大大提高了气体辐射特性的计算精度和计算速度。

参考文献:

[1] SCHENKER G N, KELLER B. Line-by-line calculation of the absorption of Infrared radiation by water vapor in a box-shaped enclosure filled with humid air[J]. International Journal of Heat and Mass Transfer, 1995, 38(17): 3127—3134.

[2] ROTHMANA L S, CAMY P C, FLAUD J M, et al. HITEMP, the high-temperature molecular spectroscopic database 2000[EB/OL]. Proceeding on line, http://www.hitran.com.

[3] EDWARDS D K. Molecular gas rand radiation[J]. In Advances in Heat Transfer, 1976, 12: 115—193.

[4] 石广玉. 大气辐射计算的吸收系数分布模式[J]. 大气科学, 1998, 22(4): 559—674.

[5] SOUFIANI A, TAINE J. High temperature gas radiative property parameters of statistical narrow-band model for H_2O, CO_2 and CO, and correlated-k model for H_2O and CO_2[J]. International Journal of Heat and Mass Transfer, 1997, 40: 987—991.

[6] MODEST M F, ZHANG H. The full-spectrum correlated-k distribution for thermal radiation from molecular gas-particulate mixtures[J]. ASME J Heat Transfer, 2002, 124: 30—38.

[7] MODEST M F. Narrow-band and full-spectrum k-distributions for radiative heat transfer-correlated-k vs. scaling approximation [J]. Journal of Quantitative Spectroscopy & Radiative Transfer, 2003, 76: 69—83.

[8] ZHANG H. Radiative properties and radiative heat transfer calculations for high temperature combustion gases[D]. Pennsylvania: The Pennsylvania State University, 2002.

[9] MODEST M F. Radiative heat transfer[M]. New York: Mcgraw-Hill Press, 2002.

[10] MARIN O, BUCKIUS R O. A simplified wide band model of the cumulative distribution function for carton dioxide [J]. International Journal of Heat and Mass Transfer, 1998, 41: 3881—3897.

[11] 聂宇宏, 陈海耿. 气体辐射宽带关联 k 模型的修正算法[J]. 计算物理, 2002, 19(5): 439—442.

[12] 聂宇宏, 陈海耿. 非灰气体的宽带吸收系数模型[J]. 东北大学学报(自然科学版), 2002, 23(4): 375—378.

(编辑 韩 锋)

新能源技术

海洋波浪气象发电机问世

苏格兰海洋能源新研发的海浪能源系统将于 2008 年正式启动,自动气象站的波浪能量转换器是一个固定于海底的圆筒形浮标,位于波浪中的充气套管随着波浪起伏套筒对浮标的圆筒缸体底部做上下运动。当一个波峰到来时,缸顶与上部浮于压缩气缸以平衡压力;相反,波峰过后缸内气体膨胀,套筒上升。苏格兰海洋能源系统将这一上下运动的动能转换成电能。自动气象站发电机与其它海洋发电技术相比具有许多优势:自动气象站被淹没在至少 6 m 以下的海底,几乎不受日照的干扰;功率较大、成本相对较低等,发展前景甚佳。

(赵旺初 供稿)

able change. The percentage of Hg^{2+} will increase from 14.71% to 39.54%, that of Hg^0 will decrease from 85.19% to 60.38% and that of Hg^P will drop from 0.10% to 0.08%. The chlorine in coal and NO_x, SO_2, HCl, Cl_2 in the flue gas assume a positive correlation to the formation of oxidized mercury in the flue gas. **Key words**: coal-fired power plant, mercury morphological distribution, flue gas

温度对 NO_2 差分吸收光谱特性影响的实验研究＝**Experimental Study of the Influence of Temperatures on NO_2 Differential Absorption Spectrum Characteristics**[刊, 汉] / SHAO Li-tang, TANG Guang-hua, XU Chuan-long, et al (Education Ministry Key Laboratory on Clean Coal Power Generation and Combustion Technology, Southeast University, Nanjing, China, Post Code: 210096)// Journal of Engineering for Thermal Energy & Power. — 2008, 23(4). —404 ~ 407

When differential optical absorption spectroscopy is applied to monitor the flue gas emissions from a fixed pollution source, the flue gas temperature will exercise a relatively great impact on the NO_2 visible ultraviolet absorption characteristics. On a self-made test stand, an experimental study has been conducted of the differential absorption spectrum characteristics of NO_2 gas when its temperature falls in a range of 30 ~ 390 ℃. The test results show that when the temperature is in a range of 30 ~ 150 ℃, the differential absorption cross section will be subjected to a leap change in the presence of a temperature rise. However, its spectrum contour will be kept unchanged. When the temperature is in a range of 150 ~ 270 ℃, a temperature rise will lead to a decrease of the differential spectrum peak value and an increase of the valley value. When the temperature is higher than 270 ℃, a conspicuous change will occur to the fine configuration of the differential absorption spectrum and the number of peaks and valleys will increase. **Key words**: differential optical absorption spectroscopy (DOAS), nitrogen dioxide (NO_2), absorption cross section, influence of temperatures

甲烷扩散火焰空间拟序结构三维运动研究＝**A Study of the Three-dimensional Movement of a Coherent Structure in a Methane Diffusion Flame Space**[刊, 汉] / HUANG Qun-xing, WANG Fei, YAN Jian-hua, et al (National Key Laboratory on Clean Utilization of Energy Source, Zhejiang University, Hangzhou, Post Code: 310027)// Journal of Engineering for Thermal Energy & Power. — 2008, 23(1). —408 ~ 412

An analytic method was presented for the three-dimensional movement characteristics of turbulent flames based on a high-speed stereoscopic visualization. The method in question first makes use of a stereoscope with dual viewing angles to enable a single CCD (charge coupled device) target surface acquiring simultaneously two flame images from different angles. Through a calibration, the parameters of a video camera can be obtained. Finally, a three-dimensional distribution of the vortex configuration in the flames and its diffusion speed can be determined by using the three-dimensional rebuilding method based on a two-eye visualization theory. Through experiments, reestablished were the three-dimensional distribution and velocity profile of the vortex configuration in a methane premixed flame. The calculation results show that due to the non-uniformity of the radial distribution of combustion speeds and the expansion action of gas flow when it is heated, the flame surface will be bent outwards near its boundary. **Key words**: turbulent flame, coherent structure, stereoscope with double viewing angles

二氧化碳气体辐射特性宽带 k 分布模型＝**A Wide-band k Distribution Model for Radiative Characteristics of Carbon Dioxide**[刊, 汉] / YIN Xue-mei, LIU Lin-hua, LI Bing-xi (College of Energy Science and Engineering, Harbin Institute of Technology, Harbin, China, Post Code: 150001)// Journal of Engineering for Thermal Energy & Power. — 2008, 23(4). —413 ~416

A novel wide-band k distribution model was established. The spectrum radiative characteristic parameters of carbon dioxide were obtained from a high-temperature gas database HITEMP. A correlation formula was used to perform a fitting of the absorption coefficient of main carbon dioxide spectrum band. The model in question was used to calculate the radiative heat flux of the carbon dioxide. A comparison was made with a line-by-line calculation method, statistical narrow-band model, a narrow-band and a full-spectrum k distribution model. The results of the comparison show that for isothermal gases, the results obtained by using the wide-band k distribution model are in very good agreement with those obtained by using the line-by-line calculation method, even more accurate than those obtained by using the full-spectrum k

distribution model. If the integration format is properly chosen, the wide-band k distribution model can attain a calculation accuracy higher than that of the statistical narrow-band model, but comparable to that of the narrow-band k distribution model. For non-isothermal gases between ash wall plates, the calculation error of the wide-band k distribution model is about 10% when its calculation results are compared with those of the line-by-line calculation method, thus greatly enhancing the calculation accuracy and speed of gas radiative characteristics. **Key words**: carbon dioxide, wide-band k distribution model, radiative heat flux

选择性非催化脱硝不同还原剂的比较试验研究＝**A Contrast and Experimental Study of Various Reduction Agents for Selective Non-catalytic Denitration Process**[刊, 汉] / LI Ke-fu, WU Shao-hua, QIN Yu-kun (Combustion Engineering Research Institute, Harbin Institute of Technology, Harbin, China, Post Code: 150001), GAO Guan-shuai, LI Zhen-zhong (Technology Research Center of National Power Plant Combustion Engineering, Shenyang, China, Post Code: 110034) // Journal of Engineering for Thermal Energy & Power. — 2008, 23(4). —417 ~ 420

An experiment of selective non-catalytic reduction (SNCR) process was performed on a CRF (Combustion Research Facility) test rig. Carbamide, ammonia water, $(NH_4)_2CO_3$ and NH_4HCO_3 were used to reduce NO_X in flue gas and a reduction agent was sprayed into the CRF furnace through an atomization nozzle. The test results show that for the reduction agents used, with an increase of NH_3/NO molar ratio, the NO reduction efficiency will gradually increase. As for the reduction agents, such as carbamide, ammonia water and $(NH_4)_2CO_3$, NH_4HCO_3 etc., which have an ammonia/nitrogen molar ratio of 1 to 2.5, the denitration efficiencies will be 65%—89%, 62%—86% and 45%—84% respectively. As regards NH_4HCO_3 which has an ammonia/nitrogen molar ratio of 0.8 to 1.5, the denitration efficiency will be 46%—73%. The temperature windows of various reduction agents are different. The reaction temperature suitable for conducting the SNCR process is the highest for carbamide and the lowest for ammonia water. **Key words**: selective non-catalytic reduction (SNCR), NO_X, reduction agent, amido

安装倾角对热声发动机性能影响的试验研究＝**An Experimental Study of the Influence of Installation Inclination Angles on Thermoacoustic Engine Performance**[刊, 汉] / SHEN Chao, HE Ya-ling, LU Jie, et al (National Key Laboratory on Multiple-phase Flow in Power Engineering, College of Energy Source and Power Engineering, Xi'an Jiaotong University, Xi'an, China, Post Code: 710049) // Journal of Engineering for Thermal Energy & Power. — 2008, 23(4). —421 ~ 424

To fully utilize solar energy as a driving heat source, an experimental study was carried out of the thermodynamic performance of a standing-wave type thermoacoustic engine installed at various inclination angles. The test results show that the installation inclination angle of the thermoacoustic engine can exercise a remarkable influence on such parameters as the vibration-initiation temperature, vibration-fading temperature of the thermoacoustic system and temperature gradient in a plate stack during the initiation of vibration etc. When the nitrogen pressure in the system has reached 1.3 MPa, at the seven angles used during the experiment, the highest vibration initiation temperature is 484 ℃ and the lowest, 428 ℃. These characteristics can provide an experimental basis for choosing an appropriate angle to lower the vibration-initiation temperature of the system. When the system is in a stable oscillation state, any change of the installation inclination angle has a relatively small influence on such thermodynamic characteristics of the system as pressure ratio and pressure vibration amplitude. These characteristics create favorable conditions for driving at different angles thermoacoustic engines operating in a stable oscillation state by utilizing an auto-tracking solar energy collector. The test results can well provide an experimental basis for the design of solar-energy-driven thermoacoustic engines. **Key words**: thermoacoustic engine, natural convection, thermodynamic characteristics, solar energy

水煤浆流经小曲率半径弯管的阻力特性研究＝**A Study of Resistance Characteristics of Coal-water Slurry Passing Through a Tube Bend with a Small Curvature Radius**[刊, 汉] / LIU Meng, CHEN Liang-yong, DUAN Yu-feng (College of Energy Source and Environment, Southeast University, Nanjing, China, Post Code: 210096) // Journal of Engineering for Thermal Energy & Power. — 2008, 23(4). —425 ~ 428

On a self-made test stand, studied were the local resistance characteristics of water-coal slurry passing through a 90° horizontal tube bend with a small curvature radius along with an analysis of the influence of various curvature radii R_c on the